Global prediction of δ_A and δ^2H-$\delta^{18}O$ evaporation slopes for lakes and soil water accounting for seasonality

J.J. Gibson[1*], S. J. Birks[2,3,], T.W.D. Edwards[3]
[1]Alberta Research Council, c/o University of Victoria, Department of Geography, P.O. Box 3050 STN CSC, Victoria BC V8W 3P5 Canada
[2]Alberta Research Council, 3608-33 Street NW, Calgary, Alberta T2L 2A6 Canada
[3]Department of Earth and Environmental Sciences, University of Waterloo, Waterloo ON N2L 3G1 Canada

Ms submitted to: Global Biogeochemical Cycles

Ms submitted on: 19 April 2007

Revised Ms submitted on: 18 January 2008

* Address for Correspondence: John Gibson (jjgibson@uvic.ca)

Global prediction of δ_A and δ^2H-$\delta^{18}O$ evaporation slopes for lakes and soil water accounting for seasonality

ABSTRACT

Global trends in the δ^2H-$\delta^{18}O$ enrichment slope of continental lakes and shallow soil water undergoing natural evaporation are predicted based on a steady-state isotope balance model using basic monthly climate data (i.e., temperature and humidity), isotopes in precipitation data, and a simple equilibrium liquid-vapour model to estimate isotopes in atmospheric moisture. The approach, which demonstrates the extension of well-known conceptual models in stable isotope hydrology to the global scale, is intended to serve as a baseline reference for evaluating field-based isotope measurements of vapour, surface water, and soil water, and as a diagnostic tool for more complex ecosystem models, including isotope-equipped climate models. Our simulations reproduce the observed local evaporation line slopes (4-5 range for lakes and 2-3 range for soil water) for South America, Africa, Australia, and Europe. A systematic increase in slopes (5-8 range for lakes) towards the high latitudes is also predicted for lakes and soil water in northern North America, Asia and Antarctica illustrating a latitudinal (mainly seasonality-related) control on the evaporation signals that has not been widely reported. The over-riding control on the poleward steepening of the local evaporation lines is found to be the isotopic separation between evaporation-flux-weighted atmospheric moisture and annual precipitation, and to lesser extents temperature and humidity, all of which are influenced by enhanced seasonality in cold regions.

INTRODUCTION

Steady-state isotope balance models have often been applied to estimate long-term average water balance conditions for lakes (*Dinçer,* 1968*; Gat,* 1995). When these models are applied in climates with a pronounced seasonality in evaporation rates, especially in environments where ice cover is present, they frequently predict slopes that differ greatly from observations. In these environments the predicted evaporative enrichment slopes are commonly lower than observed, and have therefore resulted in poor agreement between oxygen-18 and deuterium estimates of water balance parameters, or have required use (or fitting) of kinetic fractionation factors that are not in agreement with the experimental studies (*Zuber,* 1983*; Gibson et al.,* 1993). Here we present an extension to the well-known *Craig and Gordon* (1965) model of isotopic enrichment that accounts for the effects of seasonality. As the *Craig and Gordon* (1965) model is a universally applied model of the isotope exchange process during evaporation, we use it to derive reference values for evaluating sensitivity of the process to local conditions. Application of this model on a global scale provides a baseline reference for evaluating isotope-equipped models as well as providing insight into the potential labelling of atmospheric moisture sources.

One of the primary outcomes of this analysis is an awareness of the degree to which seasonality can influence evaporative enrichment, one of the most robust and distinctively labelled processes in the water cycle. Overall, we establish that for non-seasonal systems where precipitation-vapour equilibrium is assumed, it is expected that slope of the local evaporation line (LEL) for lakes is typically less than 5, and less than 3 for the upper soil layers. However, in climates with a pronounced seasonality in evaporation rates, especially in environments where ice-cover is present, the slope of the LEL depends on the open-water season temperature and relative humidity and on the isotopic separation between the annual precipitation (δ_P) and the evaporation-flux-weighted atmospheric moisture ($\delta_A^{\text{evap. fw}}$), as shown in Fig 1.

THEORY

Stable isotope tracing of evaporation and related ecosystem processes at the local, regional, and global scale requires baseline information on isotopic signatures of precipitation and atmospheric moisture, as well as general physioclimatic factors such as relative humidity and temperature that control the boundary layer structure and degree of equilibrium and kinetic isotopic fractionation (see *Gonfiantini,* 1986). While biotically-mediated vapour loss (transpiration) is generally non-fractionating (*Gat,* 1996), evaporation from open water bodies or soils produces heavy-isotope enrichment in the residual liquid and leads to a characteristic offset from the meteoric water line (MWL) in δ^2H-δ^{18}O space[1] (Fig. 1). Whereas precipitation typically clusters along the so-called Global Meteoric Water Line of *Craig* (1961) given by $\delta^2 H = 8\delta^{18} O + 10$ and hence along a slope close to 8, the stronger kinetic effects for ^{18}O relative to ^{2}H lead to evaporative enrichment of residual liquid along lines of lower slope. Deep groundwaters are expected to retain much of the isotopic signature of precipitation unless selective or episodic recharge of evaporatively enriched soil water is a locally important process in the hydrological cycle.

The isotopic composition of precipitation is controlled by a number of factors and processes, including (i) meteorological conditions (relative humidity, sea surface temperature and wind regime) controlling evaporation of water from the ocean, (ii) rainout mechanisms, which influence the fraction of precipitable water, (iii) second-order kinetic effects such as snow

[1] Isotopic ratios are reported in standard "δ" notation as deviations in per mil (‰) from Vienna-SMOW (Standard Mean Ocean Water), such that $\delta_{\text{SAMPLE}} = 1000\ ((R_{\text{SAMPLE}}/R_{\text{VSMOW}}) - 1)$, where R is $^{18}O/^{16}O$ or $^{2}H/^{1}H$.

formation or evaporation below cloud base, (iv) mixing of air masses from different oceanic source regions (*Araguás-Araguás et al.,* 2000), and (v) admixture of recycled water from evapotranspiration over the continents (*Gat,* 2000).

A simplified version of the Craig-Gordon model neglecting resistance to mixing in the liquid phase is commonly employed to describe relative changes in the isotopic composition of the evaporating flux (δ_E) and the residual liquid (δ_L) as water undergoes evaporation:

$$(1) \quad \delta_E = \frac{1}{1-h+\varepsilon_K}\left(\frac{\delta_L-\varepsilon^+}{\alpha^+} - h\delta_A - \varepsilon_K\right) \text{ (*Gonfiantini,* 1986)}$$

where h is the relative humidity; α^+ is the liquid-vapour equilibrium isotopic fractionation, estimated from empirical relations derived by *Horita and Weslowski* (1994; for δ^2H, $1000\ln\alpha^+ = 1158.8(T^3/10^9) - 1620.1(T^2/10^6) + 794.84(T/10^3) - 161.04 + 2.9992(10^9/T^3)$ and for δ^{18}O, $1000\ln\alpha^+ = 7.685 + 6.7123(10^3/T) - 1.6664(10^6/T^2) + 0.35041(10^9/T^3)$); ε^+ is the equilibrium isotopic separation between liquid and vapour, calculated as $\varepsilon^+ = (\alpha^+ - 1)$; ε_K is the equivalent kinetic isotopic separation based on wind tunnel experiments (e.g., *Vogt,* 1976; *Merlivat*, 1978; see also *Gonfiantini,* 1986), as discussed further below; and δ_A is the isotopic composition of ambient atmospheric vapour. Note that Eq. 1 is formulated for h, δ and ε values in decimal notation.

Isotopic measurements of local water vapour at ground level reveals that in most cases equilibrium is maintained between vapour and precipitation over the continents (*Araguás-Araguás et al.,* 2000), rain being the most common form of precipitation during the evaporation season. Values for the isotopic composition of δ_A have thus often been estimated based on assumed isotopic equilibrium between atmospheric moisture and precipitation (*Rozanski et al.,* 2001*; Gibson et al.,* 1993), although this hypothesis remains to be rigorously tested. *Gat et al.* (1994), *Gat and Matsui* (1991) and others have shown that isotopic composition of precipitation inherently reflects recycled moisture admixtures, including biospheric water and evaporate. Estimates of the mean annual δ_A in arid climates are more difficult to determine due to the irregular distribution of precipitation events over the course of a year.

A key diagnostic variable of mass conservation for both hydrogen and oxygen isotopes during the evaporation process is the capacity of a model to predict the observed slopes of the local evaporation lines (LELs) for soil and open water in δ^2H-δ^{18}O space. For ideal reservoirs

(either a lake or soil water pool fed by local precipitation), the slope of the LEL (S_{LEL}) predicted by the Craig-Gordon model is:

$$(2) \qquad S_{LEL} = \frac{\left[\dfrac{h(\delta_A - \delta_P) + (1+\delta_P)(\varepsilon_K + \varepsilon^+/\alpha^+)}{h - \varepsilon_K - \varepsilon^+/\alpha^+}\right]_2}{\left[\dfrac{h(\delta_A - \delta_P) + (1+\delta_P)(\varepsilon_K + \varepsilon^+/\alpha^+)}{h - \varepsilon_K - \varepsilon^+/\alpha^+}\right]_{18}}$$

where δ_A and δ_P are the isotopic compositions of atmospheric moisture and precipitation, respectively (again formulated for h, δ and ε values in decimal notation). This is sometimes termed the equilibrium evaporation slope, which applies to evaporation of local precipitation (see *Gat and Bowser,* 1991), but is distinguished from non-equilibrium evaporation slopes, which describe evaporation of allochthonous water sources, i.e., waters introduced by long-distance river transport, regional groundwater flow, or artificial diversions. Local evaporation lines (LELs) have been widely reported from field studies of water bodies (e.g., *Dinçer,* 1968*; Zuber,* 1983*; Gibson,* 2002*; Gibson et al.,* 1993, 2005) and soil water (e.g., *Barnes and Allison,* 1988; *Allison et al.,* 1983). In general, soil-water LELs have been reported as having lower slopes than open water LELs, attributed to vapour transport through the stagnant, diffusion-dominated soil matrix. Turbulence associated with evaporation from open-water surfaces under typical wind conditions reduces kinetic fractionation by half (*Gat,* 1996).

Observed LEL slopes for water bodies typically range from 4.0 to 5.5 for most regions, although studies in Arctic Canada have suggested a systematic poleward steepening of the local evaporation lines (see *Gibson et al.,* 2005), while soil-water LEL slopes are generally less than 3.

Previous studies have applied Eq. 2 to predict LEL conditions relevant to local study sites, but the approach has not been previously applied at a regional or global scale largely due to lack of available information on the isotopic composition of atmospheric moisture.

METHOD

To develop a better understanding of potential regional variations in slopes that influence labelling of evaporated water we apply Eq. 1 to station data on a global scale, incorporating

evaporation-flux-weighting as a means to account for seasonality. In this analysis precipitation is used as a systematic proxy for the isotopic composition of atmospheric moisture. Values for δ_A were determined using the precipitation-equilibrium assumption:

(3) $$\delta_A = (\delta_P - \varepsilon^+) / \alpha^+$$

Because evaporation (E) occurs under seasonally variable environmental conditions, the exchange terms δ_A, ε^+, ε_K, and h in Eq. 2 were evaluated on a monthly time-step and evaporation-flux-weighted to simulate the expected annual δ^2H-δ^{18}O trajectories. At the same time the annual precipitation δ_P values were amount-weighted from monthly data as these are expected to mimic the annual average source water to lakes and soil water. The analysis was conducted globally for terrestrial surfaces to derive annual δ_A climatologies for both δ^2H and δ^{18}O. For each tracer the ε^+ values were derived using the equations of *Horita and Wesolowski* (1994), as noted above, and ε_K values were based on $\varepsilon_K = n C_\kappa^o \theta(1-h)$ where C_κ^o is 25.0‰ and 28.6‰ for deuterium and oxygen-18, respectively, *n=1/2* for open water bodies and *n=1* for soil water, and $\theta = (1-h')/(1-h)$ is an advection term to account for the potential influence of humidity buildup, h' being the adjusted humidity of the downwind atmosphere following admixture of evaporating moisture over the surface, often set to $\theta \approx 1$ for small water bodies (*Vogt,* 1976*; Gonfiantini;* 1986*; Gat,* 1996).

The global isotope climatology used here is based on station data used to assemble a gridded precipitation dataset by *Birks et al.* (2002), but also includes additional station data from the Siberian Network for Isotopes in Precipitation (SNIP) (Fig. 2a) (*Kurita et al.*, 2004). The NCEP/NCAR reanalysis dataset (*Kalnay et al.,* 1996) was used to obtain monthly climatologies of *T*, *h* and *E* for each of the stations used in this analysis. These values were extracted from 2.5° x 2.5° grid cells and consequently may not be representative of conditions at point locations within each grid, particularly in areas of high relief and for grid cells adjacent to oceans. As a sensititvity test, S_{LEL} values were calculated using Eq. 2 and a variety of different estimates for *T*, *h* and *E* so that comparisons between S_{LEL} values obtained using different values for each of these parameters could be made. Included in our comparisons were runs made with different estimates of *T* (surface, 2m and 1000 mbar), *h* (calculated using temperature and specific humidity, and 1000 mbar relative humidity) and *E* (potential evaporation rate and latent heat flux, which are available directly as reanalysis products, as well as calculated potential *E,* based on *T* and *h*).

The calculated S_{LEL} values using these different combinations of parameters retained the general relationship between S_{LEL} and latitude, as well as the range of S_{LEL} values, regardless of which of the estimates of T, h and E were used, but differed in the number of outliers (unrealistic $S_{LEL} < 0$). Closer inspection of outliers revealed that they were primarily high-elevation stations, where all of our reanalysis-based h estimates were significantly larger than station-measured climate normals. Six such stations were removed from the dataset. The figures we present are based on the S_{LEL} estimates using potential E calculated using 2m temperatures and 1000 mbar h. Note that no additional ice freeze-over or break-up masks are applied to depict the occurrence of the open-water period, although precise timing of these events might be a potentially important modifier of environmental conditions during individual spring/fall months in high-latitude or high-altitude systems. Because these months also tend to have lower evaporation rates (at least for small lakes) it was assumed for the purposes of this analysis that the annual flux-weighting would not be significantly affected by disregarding the intra-month timing of these processes. To gain a better appreciation of the spatial variations in the estimates of S_{LEL}, δ_A and δ_P the values determined for each of the stations were interpolated onto a 2.5° x 2.5° grid using a Cressman objective analysis, a spheres of influence method developed for interpolating meteoric data (Cressman, 1959).

RESULTS

Maps illustrating $\delta^{18}O$ results for atmospheric moisture include: amount-weighted mean annual $\delta^{18}O$ of precipitation (Fig. 2a), the atmospheric moisture $\delta^{18}O$ assuming equilibrium with precipitation without monthly evaporation-flux-weighting (Fig. 2b), and finally the $\delta^{18}O$ of atmospheric moisture with monthly evaporation-flux-weighting (Fig. 2c). Maps illustrating the predicted slope of evaporation lines include: ideal precipitation-fed lakes under turbulent rough surface conditions (Fig. 3a), precipitation-fed soil water with purely diffusive water transport (Fig. 3b). Intermediate slope values would be expected for the situation of smooth open-water conditions, not common in most natural system (not shown). The predicted slope values for each of the stations used in the maps in Fig. 3 are presented in Figs. 4a-c. The effect of flux-weighting becomes apparent in Fig. 4a where slopes were calculated using Eq. 2 and annual average values of δ_A, ε^+, ε_K and h, instead of values representative of the open water season. When these parameters are flux-weighted (Figs. 4 b and c) regional differences in slopes become apparent.

Evaporation-flux-weighting the variables in Eq. 2 gives estimates of δ_A, ε^+, ε_K, and h that reflect the values most representative of periods when lakes undergo evaporation. A comparison with available observations of the evaporation slopes reported elsewhere are given in Table 1 and shown for comparison in Fig 4. Note that the poleward steepening in predicted slopes in the flux-weighted scenario appears to be a better match to the observations. It is important to note also that this poleward steepening cannot be attributed to uncertainties in estimating relative humidity at high latitudes, which can occur due to instrumental bias at very low temperatures (*New et al.*, 1999), since overestimation of h in these areas would result in a decrease in the calculated slopes at high latitudes, rather than this increasing trend.

DISCUSSION

While the use of evaporation flux-weighting for δ_A - δ_P separation remains to be rigorously tested, the new conceptual model is capable of simulating the observed steepening of the LELs at higher latitudes while using a consistent set of exchange parameters. Lower slopes predicted by the original conceptual model at high latitudes (e.g. Fig. 4a) are evidently due to improper (or lack of) weighting for the δ_A - δ_P separation, which does not account for the fact that evaporation and isotope exchange does not occur during periods of ice cover or that the process is seasonally variable. The effects of evaporation-flux-weighting on the δ_A - δ_P separation is clearly illustrated in δ^2H-δ^{18}O space (Fig. 5) where accounting for the timing of the evaporation flux during the season results in a compression of the δ_A values (Fig. 5c) that surface and soil waters equilibrate with over the active period when compared with the annual average δ_A values (Fig. 5b) encountered over the entire year. Regions where flux-weighting has the greatest influence are those with the greatest seasonality, as evident in Figs. 6a and 6b.

An interesting point that is particularly relevant to paleoclimate studies is that temporal changes in seasonality may have altered the slope of the local evaporation in the past. Application of dual oxygen-18 and deuterium tracers to lake sediment archives may therefore be able to trace changes in paleoslope of the evaporation line and provide a basis for examining past seasonality signals. For modern water balance applications, the use of non-weighted atmospheric moisture values and standard exchange parameters can result in substantial errors in computed long-term values for evaporation-to-inflow ratios, particularly for strongly seasonal climates where errors may be as high as 50% for low-throughflow/high-evaporation lakes.

Based on our model of the effects of seasonality on the isotopic labelling of evaporation, we would expect the slope of local evaporation lines to vary globally with lower values near the equator and higher values at high latitudes and altitudes, providing a readily testable hypothesis by spatial surveys of stable isotopes in lakewater. Our model predicts lakes in mid-latitude regions to have slopes ranging from 4-5, which is consistent with the ranges reported for lakes in most regions of the world (Table 1, see also Fig. 4). The only high-latitude data available are for the Canadian Arctic and Siberia where the reported $\delta^{18}O$ and $\delta^{2}H$ values result in LELs with slopes > 5 are also predicted by our modelling (Table 1). This trend has already been noted in northern Canada (*Gibson et al.,* 2005). There are relatively fewer soil water $\delta^{18}O$ and $\delta^{2}H$ data available to compare with our modelled estimates. With the exception of fairly high soil water slopes reported by *Darling and Bath* (1988) the slopes found for soil water are systematically lower than those reported for surface waters as our model predicts.

The reason for the poleward steepening of the predicted LEL slopes becomes evident with closer examination of Eq. (2). The humidity dependence of S_{LEL} varies with the seasonality of the system. Seasonality results in compression of the apparent separation between δ_A and δ_P to values much less than ε^+ (shown schematically in Fig. 1). In non-seasonal climates evaporation from water bodies is distributed equally over the entire year. This is in stark contrast to highly seasonal climates, which have a strong bias in the timing of evaporation. In extreme cases such as at very high latitudes, frozen conditions can effectively isolate water bodies from the atmosphere for greater than 10 months of the year. Flux-weighting the transfer terms by evaporation effectively accounts for the greater importance of meteorological conditions during periods when the majority of evaporation is occurring, instead of relying on annual averages. In seasonal climates the weighted mean annual composition of precipitation (δ_P) will still likely be the starting point for evaporation for lakes and soil water, however, the atmospheric moisture (δ_A) to which the evaporating water body is exposed will be representative of the evaporation-flux-weighted δ_A (see Fig. 2). In addition, the evaporation will occur under relative humidity and temperature conditions representative of the evaporative season, not the entire year (Fig 7).

IMPLICATIONS

Quantifying the offset of lakes and rivers from the MWL along LELs has been used within the context of an isotope-mass balance analysis to partition water budget components,

whereby fractionating losses (e.g., open-water evaporation) are distinguished from non-fractionating losses (e.g., liquid outflow or transpiration). The dual-tracer approach, using both ^{2}H and ^{18}O has generally been most successful in this application due to the ability to positively identify open-water evaporation effects in the residual liquid as described above, but also for its ability to constrain errors, or unknown water budget components such as the isotope composition of atmospheric moisture, or kinetic fractionation factors. An evolution of practical approaches has been demonstrated over time (see *Gibson et al.*, 2005). For a simple open-water body with liquid outflow and evaporation, the fraction of evaporation losses can be estimated for each tracer from the isotopic offset in the residual liquid as

$$E/I = (\delta_P - \delta_L)/(\delta_E - \delta_L) \quad (4)$$

where δ_P, δ_L and δ_E are the isotopic compositions of precipitation, lake water and evaporate, respectively, and I is the isotopic composition of local precipitation-derived inflow. Due to practical difficulties in direct sampling of δ_E, this value is commonly characterized indirectly based on knowledge of the boundary layer conditions using the Craig-Gordon model (Eq. 1). For systems in which evaporation and transpiration are both significant, outflow gauging records can be used to partition the non-evaporated fraction between transpiration losses and liquid outflows (see *Gibson et al.*, 2005).

The effect of seasonality on the slope of local evaporation lines has implications for the partitioning of evaporation and transpiration using water isotope tracers. A variety of conceptual isotopic labelling scenarios are given for an idealized evapotranspiring system comprising lakes or storage reservoirs and vegetated transpiring land surfaces in various climatic situations (Fig. 8 a-c). As shown, the seasonality effect has little impact on the predicted LEL slopes at low latitudes (Fig. 8a), with both the Craig-Gordon model and our seasonal model predicting slopes of about 4. Lakes in these regions are typically close to isotopic steady-state, so that δ_E tends to be similar to δ_P. While liquid water partitioning is therefore likely to be successful, the vapour fluxes δ_E and δ_T are likely to be poorly distinguished with both being approximately equal to the mean annual δ_P composition, resulting in a situation where one should expect little potential for vapour partitioning using isotope tracers on an annual time-scale. Short-term variations may still produce significant temporal offsets, but on the long-term these differences are likely to diminish.

The situation changes in mid-latitude regions where lakes are less likely to reach isotopic steady-state (Fig. 8b). Our seasonal conceptual model predicts that slopes of local evaporation

lines in these setting should be slightly steeper (5-6) than predicted by the Craig-Gordon model (~ 4). In these areas the δ_E produced from evaporating surface waters will be isotopically distinct from precipitation and transpiration because the slopes of the LELs should be sufficiently different from the local meteoric water line if the lakes are not at isotopic steady-state. Transpiration in these settings will resemble weighted mean annual precipitation and the isotopic difference between δ_E and δ_T suggests there should be potential for partitioning these fluxes using isotope tracers both in the residual liquid and in the vapour phase.

For high-latitude regions with highly seasonal climates our model suggests that the slopes of the LEL will at some point approach the slope of most MWLs (~ 8), creating a situation where the LEL is co-linear with the MWL and δ_E, δ_T and δ_P all appear to plot on an apparent MWL. The similarity between the slopes of the LEL and MWL would make detecting evaporative enrichment effects and partitioning evaporation and transpiration more difficult, especially in the liquid phase. It is important to clarify that isotopic detection of evaporate and transpirate in the vapour phase should still be possible at extreme high-latitudes as δ_E and δ_T are not expected to be identical. The tendency toward co-linearity at high-latitudes may however diminish the value of applying the dual tracer approach, although this remains to be verified.

Table 1: Summary of published S_{LEL} values for surface waters and soil waters.

Location (surface water)	Observed $S_{LELsurface\ water}$	Reference	Location (soil water)	Observed $S_{LELsoil\ water}$	Reference
North America			**North America**		
>60	4.8-7.1	(*Gibson et al.,* 2005)	NWT	4.7	based on data from *Stewart* (1994)
<60	4.1-4.7		Saskatchewan	4.46	(*Maule*, 1994)
Greenland					
Close to icesheet coastal	3.9 4.9-5.6	(*Leng and Anderson,* 2003)			
Europe			**Europe**		
Germany	5	(*von Grafenstein,* 2002)	UK	5.7 to 6.4	(*Darling and Bath*, 1988)
Austria	4.4	(*Yehdegho et al.,* 1997)			
Switzerland	5.1	(*Teranes and McKenzie,* 2001)			
Poland	5	(*Zuber,* 1983)			
Scandinavia					
Southern Sweden	4.9	(*Hammarlund et al.,* 2003)			
Siberia					
Taimyr Peninsula	6.8	(*Wolfe and Edwards,* 1997)			
Turkey					
Egridir and Beysehir	5	(*Dinçer,* 1968)			
South America					
Andes	5.1	(*Wolfe et al.,* 2001)			
Africa			**Africa**		
Sahel Lakes	4.6	(*Fontes and Gonfiantini,* 1967)	Sahara	2	(*Dinçer et al.,* 1974)
Mt. Menka	4.6	(*Rietti-Shati et al.,* 2000)			
Australia			**Australia**		
Western	4.3-4.6	(*Hamilton et al.,* 2005)		3.7 to 5.4	(*Allison and Hughes,* 1983)
Queensland	3.9	(*Turner et al.,* 1984)		2.7 to 3.5	(*Allison et al.,* 1983)
South Australia					
Asia					
Western Tibet	3.5	(*Fontes et al.,* 1996)			
Western China	3.3	(*Yang et al.,* 1995) saline			

REFERENCES:

Allison, G.B., C.J. Barnes, M.W. Hughes, and F.W.J. Leaney (1983), Effect of climate and vegetation on oxygen-18 and deuterium profiles in soils, in *Proceedings IAEA Isotope Hydrology*, pp. 105-123, Vienna.

Allison, G.B., and M.W. Hughes (1983), The use of natural tracers as indicators of soil-water movement in a temperate semi-arid region, *Journal of Hydrology*, *60* (157-173).

Araguás-Araguás , L., K. Froehlich, and K. Rozanski (2000), Deuterium and oxygen-18 isotope composition of precipitation and atmospheric moisture, *Hydrological Processes*, *14* (8), 1341-1355.

Barnes, C.J., and G.B. Allison (1988), Tracing of water movement in the unsaturated zone using stable isotopes of hydrogen and oxygen, *Journal of Hydrology*, *100*, 143-176.

Birks, S.J., J.J. Gibson, L. Gourcy, P.K. Aggarwal, and T.W.D. Edwards (2002), Maps and animations offer new opportunities for studying the global water cycle, *Eos*, Electron. Suppl., 83, http://www.agu.org/eos_elec/020082e.html.

Craig, H. (1961), Isotopic variations in meteoric waters, *Science*, *133*, 1702-1703.

Craig, H., and L. Gordon (1965), Deuterium and oxygen-18 in the ocean and the marine atmosphere, in *Stable Isotopes in Oceanographic Studies and Paleotemperatures*, edited by E. Tongiorgi, pp. 9-130, Spoleto.

Cressman, G.P., 1959. An operational objective analysis system. *Monthly Weather Review* 87, 367-374.

Darling, W.G., and A.H. Bath (1988), A stable isotope study of recharge processes in the English chalk, *Journal of Hydrology*, *101*, 31-46.

Dinçer, T. (1968), The use of oxygen-18 and deuterium concentrations in the water balance of lakes, *Water Resources Research*, *4*, 1289-1305.

Dinçer, T., A. AI-Mugrin, and U. Zimmermann (1974), Study of the infiltration and recharge through the sand dunes in arid zones with special reference to the stable isotopes and thermonuclear tritium, *Journal of Hydrology*, *23*, 79-109.

Fontes, J.C., F. Gasse, and E. Gibert (1996), Holocene environmental changes in Lake Bangong Basin (Western Tibet). Part 1: Chronology and stable isotopes of carbonates of a Holocene lacustrine core, *Palaeogeography Palaeoclimatology Palaeoecology*, *120*, 25-47.

Fontes, J.C., and R. Gonfiantini (1967), Comportement isotopique au cours de l'evporation de deux bassins sahariens, *Earth and Planetary Science Letters*, *3*, 258-266.

Gat, J.R. (1995), Stable isotopes of fresh and saline lakes, in *Physics and Chemistry of Lakes*, edited by A. Lerman, D. Imboden, and J.R. Gat, pp. 139-165, Springer-Verlag, Berlin.

Gat, J.R. (1996), Oxygen and hydrogen isotopes in the hydrologic cycle, *Annual Review of Earth and Planetary Sciences*, *24*, 225-262.

Gat, J.R. (2000), Atmospheric water balance - the isotopic perspective, *Hydrological Processes*, *14* (8), 1357-1369.

Gat, J.R., C.J. Bowser, and C. Kendall (1994), The contribution of evaporation from the Great Lakes to the continental atmosphere: estimate based on stable isotope data, *Geophysical Research Letters*, *21* (7), 557-560.

Gat, J.R., and E. Matsui (1991), Atmospheric water balance in the Amazon Basin: an isotopic evapotranspiration model, *Journal of Geophysical Research*, *96* (D7), 13,179-13,188.

Gibson, J.J. (2002), Short-term evaporation and water budget comparisons in shallow arctic lakes using non-steady isotope mass balance, *Journal of Hydrology*, *264*, 247-266.

Gibson, J.J., T.W.D. Edwards, S.J. Birks, N.A. St. Amour, W.M. Buhay, P. McEachern, B.B. Wolfe, and D.L. Peters (2005), Progress in isotope tracer hydrology in Canada, *Hydrological Processes*, *19*, 303-327.

Gibson, J.J., T.W.D. Edwards, G.G. Bursey, and T.D. Prowse (1993), Estimating evaporation using stable isotopes; quantitative results and sensitivity analysis for two catchments in northern Canada, *Nordic Hydrology*, *24* (2-3), 79-94.

Gibson, J.J., E.E. Prepas, and P. McEachern (2002), Quantitative comparison of lake throughflow, residency, and catchment runoff using stable isotopes: modelling and results from a survey of boreal lakes, *Journal of Hydrology*, *262*, 128-144.

Gonfiantini, R. (1986), Environmental isotopes in lake studies, in *Handbook of Environmental Isotope Geochemistry*, edited by P. Fritz, and J.C. Fontes, pp. 113-168, Elsevier, New York.

Hamilton, S.K., S.E. Bunn, M.C. Thoms, and J.C. Marshall (2005), Persistence of aquatic refugia between flow pulses in a dryland river system, *Limnology and Oceanography*, *50* (3), 743-754.

Hammarlund, D., S. Bjorck, B. Buchardt, C. Israelson, and C.T. Thomsen (2003), Rapid hydrological changes during the Holocene revealed by stable isotope records of lacustrine carbonates from Lake Igelsjon, southern Sweden, *Quaternary Science Reviews*, *22*, 353-379.

Horita, J., and D. Wesolowski (1994), Liquid-vapour fractionation of oxygen and hydrogen isotopes of water from the freezing to the critical temperature, *Geochimica et Cosmochimica Acta*, *58*, 3425-3437.

Kalnay, E., M. Kanamitsu, R. Kistler, W. Collins, D. Deavan, L. Gandin, M. Iredell, S. Saha, G. White, J. Woollen, Y. Zhu, M. Chelliah, W. Ebisuzaki, W. Higgins, J. Janowiak, K.C. Mo, C. Ropelewski, J. Wang, A. Leetma, R. Reynolds, R. Jenne, and D. Joseph (1996), The NCEP/NCAR 40-year reanalysis project, *Bulletin of the American Meteorological Society*, *77*, 437-471.

Kurita, N., N. Yoshida, G. Inoue, and E.A. Chayanova (2004), Modern isotope climatology of Russia: A first assessment, *Journal of Geophysical Research*, *109* (D03102), doi:10.1029/2003JD003404.

Leng, M.J., and N.J. Anderson (2003), Isotopic variation in modern lake waters from western Greenland, *The Holocene*, *13* (4), 605-611.

Maulé, C., D.S. Chanasyk, and K. Muehlenbachs (1994), Isotopic determination of snow-water contribution to soil water and groundwater, *Journal of Hydrology*, *155*, 73-91.

Merlivat, L. (1978), Molecular diffusivities of $H_2{}^{16}O$, $HD^{16}O$, and $H_2{}^{18}O$ in gases, *Journal of Chemical Physics, 69* (6), 2864-2871.

New, M., M. Hulme, and P. Jones (1999), Representing Twentieth-Century Space–Time Climate Variability. Part I: Development of a 1961–90 Mean Monthly Terrestrial Climatology, *Journal of Climate*, *12* (3), 829-856.

Rietti-Shati, M., R. Yam, W. Karlen, and A. Shemesh (2000), Stable isotope composition of tropical high-altitude fresh-waters on Mt. Kenya, Equatorial East Africa, *Chemical Geology*, *166*, 341-350.

Rozanski, K., K. Froehlich, and W.G. Mook (2001), Surface water, in *Environmental isotopes in the hydrological cycle: Principles and applications*, edited by W.G. Mook, pp. 117.

Stewart, C.L. (1994), An isotopic investigation of passive dewatering of tailings at the Lupin Mine site, Northwest Territories,, BASc thesis, University of Waterloo.

Teranes, J.L., and J.A. McKenzie (2001), Lacustrine oxygen isotope record of 20th-century climate change in central Europe: evaluation of climatic controls on oxygen isotopes in precipitation, *Journal of Paleolimnology*, *26* (2), 131-146.

Turner, J.V., G.B. Allison, and J.W. Holmes (1984), The water balance of a small lake using stable isotopes and tritium, *Journal of Hydrology*, *70*, 199-220.

Vogt, H.J. (1976), Isotopentrennung bei der Verdampfung von Wasser, Universitat Heidelberg.

von Grafenstein, U. (2002), Oxygen-isotope studies of ostracods from deep lakes, *Geophysical Monograph, The Ostracoda: Applications in Quaternary Research*, *131*, 249-266.

Wolfe, B.B., and T.W.D. Edwards (1997), Hydrologic control on the oxygen-isotope relation between sediment cellulose and lake water, western Taimyr Peninsula, Russia; implications for the use of surface-sediment calibrations in paleolimnology, *Journal of Paleolimnology*, *18* (3), 283-291.

Wolfe, B.B., T.W.D. Edwards, K.R.M. Beuning, and R.J. Elgood (2001), Carbon and oxygen isotope analysis of lake sediment cellulose: methods and applications, in *Tracking Environmental Change Using Lake Sediments: Physical and Chemical Techniques, Developments in Paleoenvironmental Research*, edited by W.M. Last, and J.P. Smol, pp. 373-400, Kluwer Academic Publishers, Dordrecht, The Netherlands.

Yang, W., R.J. Spencer, H.R. Krouse, T.K. Lowenstein, and E. Casas (1995), Stable isotopes of lake and fluid inclusion brines, Dabusun Lake, Qaidam Basin, western China: Hydrology and paleoclimatology in arid environments, *Palaeogeography Palaeoclimatology Palaeoecology*, *117*, 279-290.

Yehdegho, B., K. Rozanski, H. Zojer, and W. Stichler (1997), Interaction of dredging lakes with the adjacent groundwater field; an isotope study, *Journal of Hydrology*, *192* (1-4), 247-270.

Zuber, A. (1983), On the environmental isotope method for determining the water balance componenets of some lakes, *Journal of Hydrology*, *61*, 409-427.

Figure Captions

Figure 1: δ^2H-δ^{18}O plots showing the conceptual model of evaporative isotope enrichment (a) for a non-seasonal climate with constant monthly evaporation rate, assuming precipitation-vapour isotopic equilibrium, and (b) for a seasonal climate with variable monthly evaporation rate, assuming precipitation is evaporation-flux-weighted. Note that the isotopic separation between the effective long-term liquid and vapour is less than equilibrium in (b) due to the seasonality effect (i.e., $\delta_P^{annual} - \delta_A^{evap.fw} < \varepsilon^+$). Note that ε^+ is evaluated at annual and monthly flux-weighted temperature for (a) and (b), respectively.

Figure 2:. Plots of δ^{18}O in the following: (a) mean annual amount-weighted precipitation based on monthly data of *Birks et al.* (2002) with additional data from SNIP (*Kurita et al.*, 2004), (b) mean annual atmospheric moisture composition assuming liquid-vapour equilibrium with annual precipitation above, and (c) evaporation-flux-weighted atmospheric moisture assuming liquid-vapour equilibrium.

Figure 3 Modelled slopes of equilibrium local evaporation lines calculated for (a) surface waters and (b) soil water.

Figure 4: Slopes calculated using Equation 2 for each of the GNIP (filled symbols) and SNIP (open symbols) stations, compared to observations compiled from table 1 (cross symbols). In (a) average annual values of δ_A, ε^+, ε_K, and h are used in the calculations, producing a fairly uniform predicted slope regardless of latitude. When the same calculations are performed using evaporation-flux-weighted values a pronounced steepening of the predicted S_{LEL} for (b) lakes and (c) soil water becomes apparent.

Figure 5: a) The δ^2H-δ^{18}O relationship for precipitation (δ_P) for all stations contained in the GNIP and SNIP datasets plotted with the modelled atmospheric water vapour (δ_A) and the Global Meteoric Water Line (GMWL). Examining the calculated δ_A values without (b) and with (c) evaporation flux-weighting illustrates the importance of seasonality in determining the ambient atmospheric conditions when surface water evaporates.

Figure 6: The regions where evaporation-flux-weighting has the largest influence becomes apparent in (a) the latitudinal distribution of $(\delta_P-\delta_A)/\varepsilon^+$ and in (b) the difference between the average annual δ_A of water vapour δ^{18}O and the evaporation-flux-weighted average water vapour ($\delta_A^{evap.\ fw}$). Note that ε^+ in (a) is evaluated using annual temperature.

Figure 7: The effects of evaporation flux-weighting are evident in comparisons of predicted S_{LEL} and temperature (a-b), relative humidity (c-d) and for ^{18}O, the separation between δ_P and δ_A (e) and the evaporation flux-weighted separation normalized to the predicted equilibrium separation for ^{18}O (f). Evaporation flux-weighting results in the flux-weighted temperatures being significantly higher than the seasonal averages. In regions having high S_{LEL} the flux-weighted relative humidities are higher than the seasonal averages. The separation between weighted mean annual precipitation δ_P and the equilibrium predicted δ_A is greatest in regions with the highest S_{LEL} (e). The greatest deviation between the flux-weighted separation and predicted separation

also occurs in regions with the highest slopes (f). Note that ε_{18}^{+} is an estimate for ^{18}O based on annual temperature.

Figure 8: Conceptual model showing the effects of seasonality on the isotopic labelling of evaporation (δ_E) and transpiration (δ_T) and the potential for using isotopic labelling to distinguish between the two fluxes. At low latitudes (a) δ_E and δ_T will be poorly labelled as both will be very similar to the mean annual δ_P values. In mid-latitude regions (b) there is a much better potential for isotopic labelling and separation of the evaporation and transpiration fluxes. At very high latitudes (c) the steepening of the LEL results in a situation where the evaporative flux will be indistinguishable isotopically from transpired moisture and precipitation due to similarity of the MWL and LEL slopes. Note that ε^{+} depicts the monthly flux-weighted value which is indistinguishable from the annual value for the idealized low-latitude scenario shown in (a).

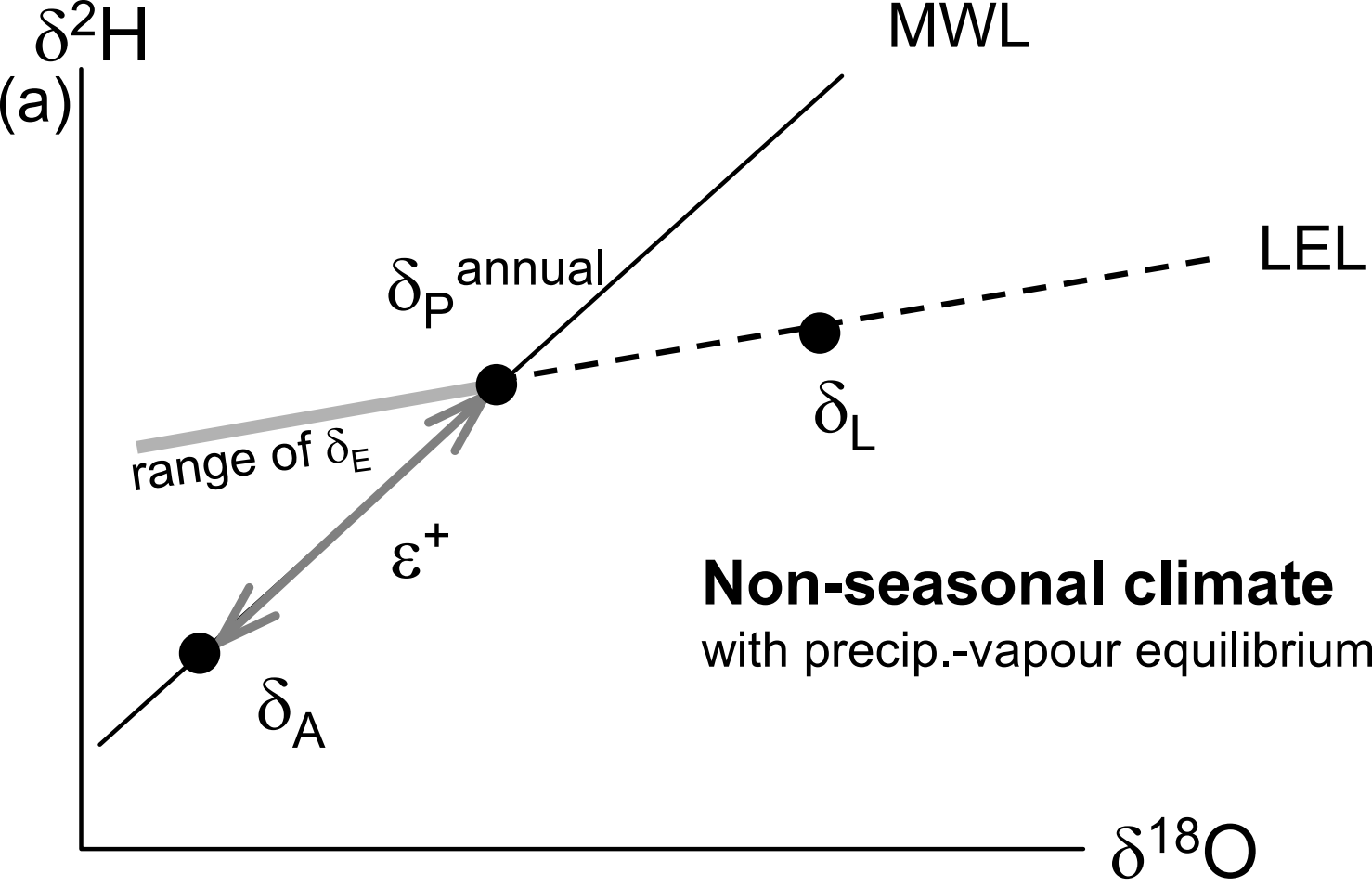
δ2H
(a)
MWL
LEL
δP annual
δL
range of δE
ε+
δA
Non-seasonal climate
with precip.-vapour equilibrium
δ18O

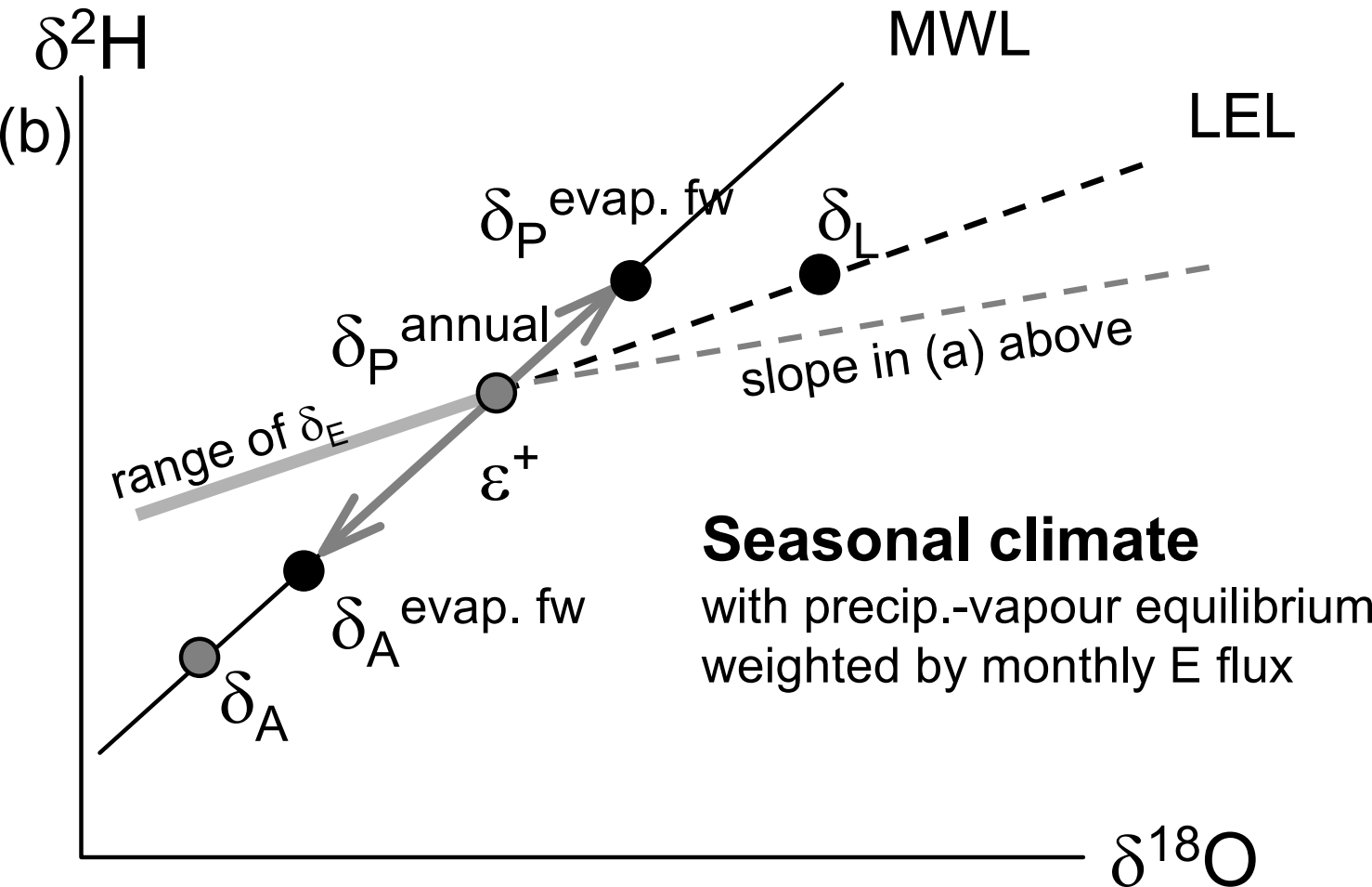
δ2H
(b)
MWL
LEL
δP evap. fw
δL
δP annual
slope in (a) above
range of δE
ε+
δA evap. fw
δA
Seasonal climate
with precip.-vapour equilibrium
weighted by monthly E flux
δ18O

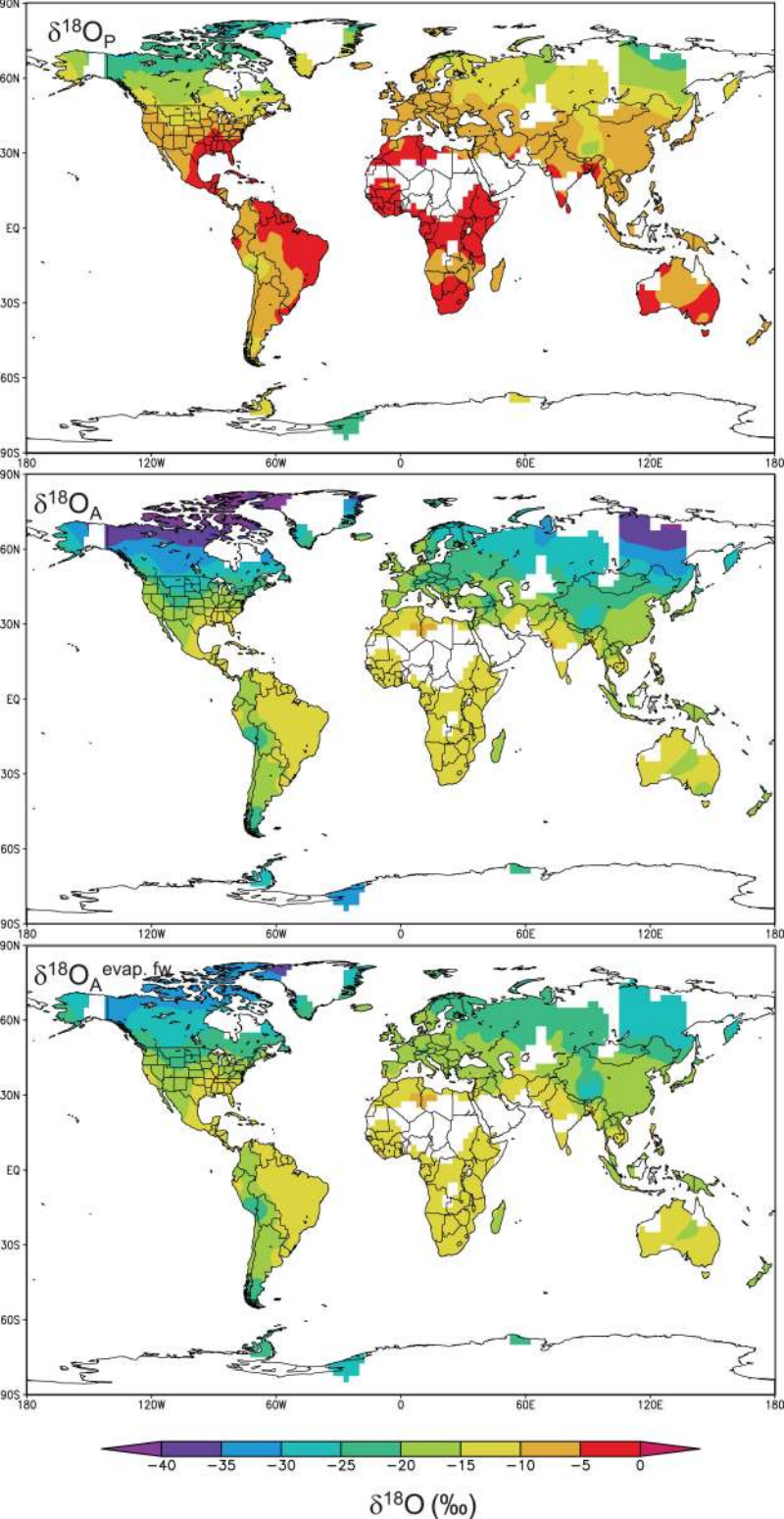
δ18OP
δ18OA
δ18OA evap. fw
90N
60N
30N
EQ
30S
60S
90S
180
120W
60W
0
60E
120E
180
−40
−35
−30
−25
−20
−15
−10
−5
0
δ18O (‰)

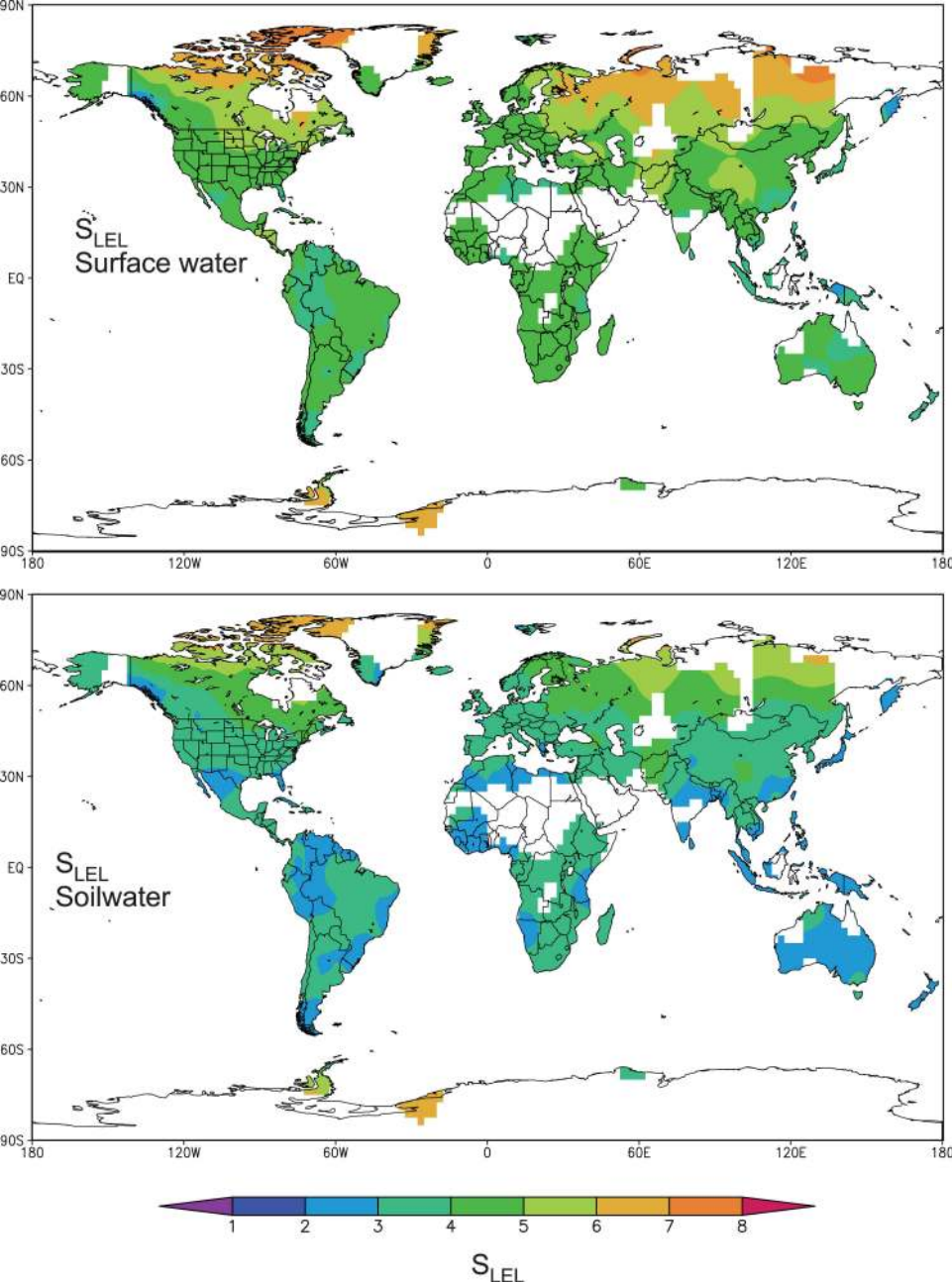
S_{LEL}
Surface water
S_{LEL}
Soilwater
90N
60N
30N
EQ
30S
60S
90S
180
120W
60W
0
60E
120E
180
1
2
3
4
5
6
7
8
S_{LEL}

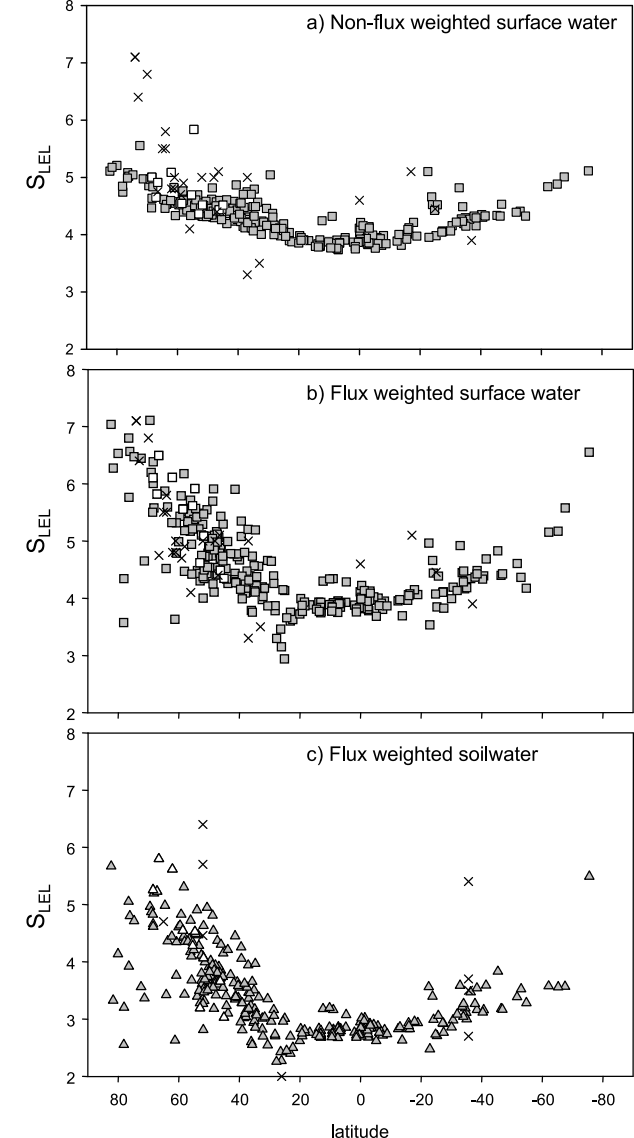
a) Non-flux weighted surface water
b) Flux weighted surface water
c) Flux weighted soilwater
S_{LEL}
8
7
6
5
4
3
2
80
60
40
20
0
-20
-40
-60
-80
latitude

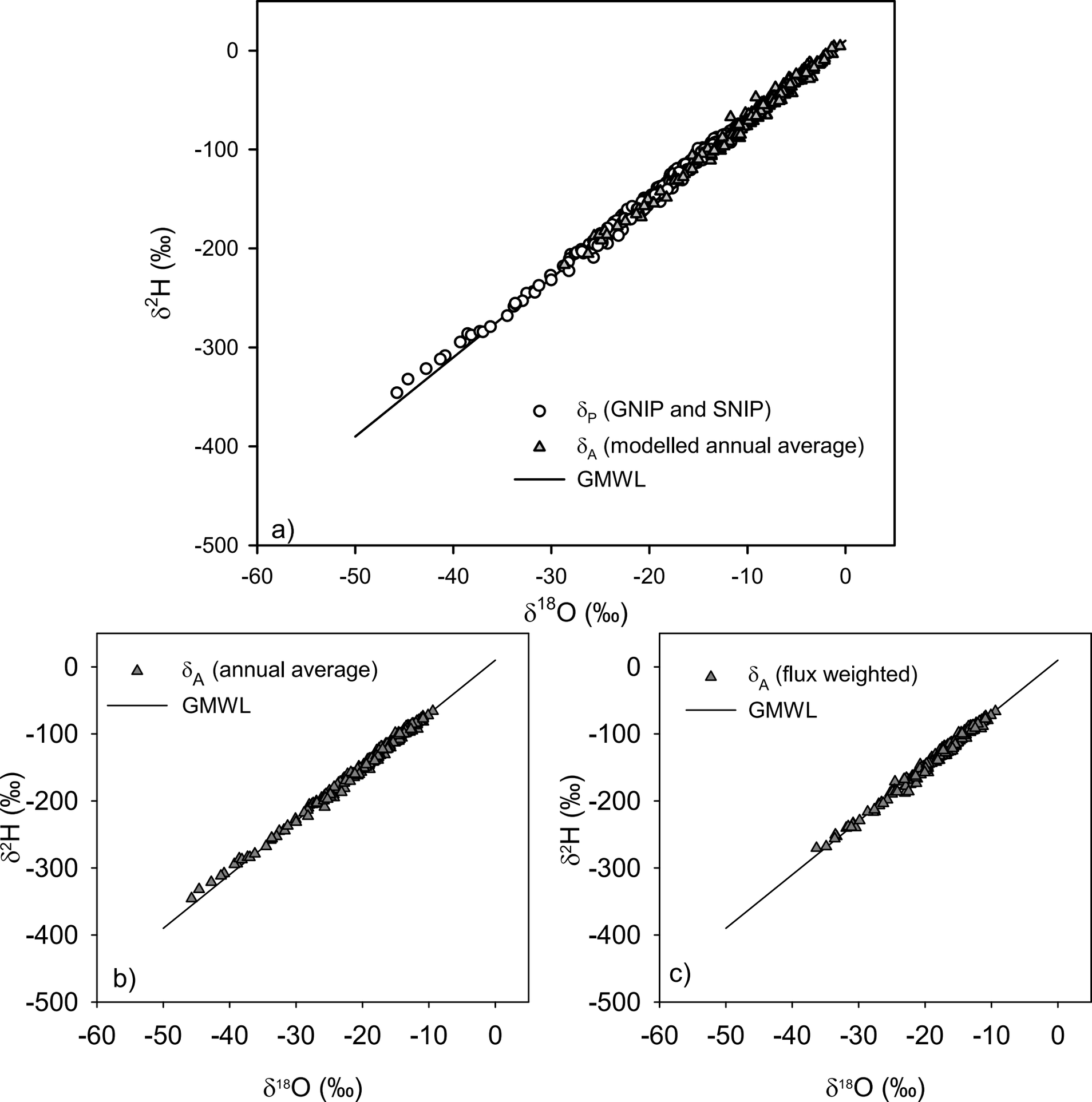
0
-100
-200
-300
-400
-500
δ²H (‰)
-60
-50
-40
-30
-20
-10
0
δ¹⁸O (‰)
δP (GNIP and SNIP)
δA (modelled annual average)
GMWL
a)
δA (annual average)
GMWL
b)
δA (flux weighted)
GMWL
c)

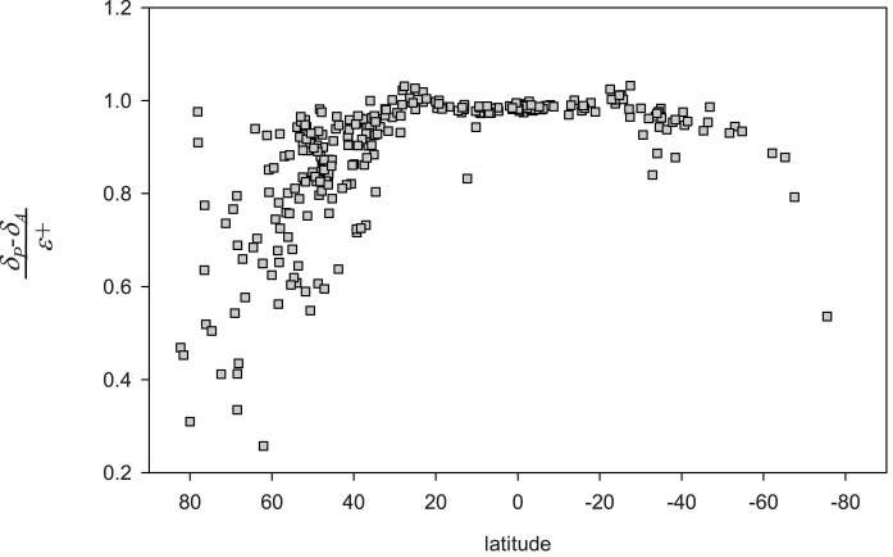
1.2
1.0
0.8
0.6
0.4
0.2
$\frac{\delta_p - \delta_A}{\varepsilon^+}$
80
60
40
20
0
-20
-40
-60
-80
latitude

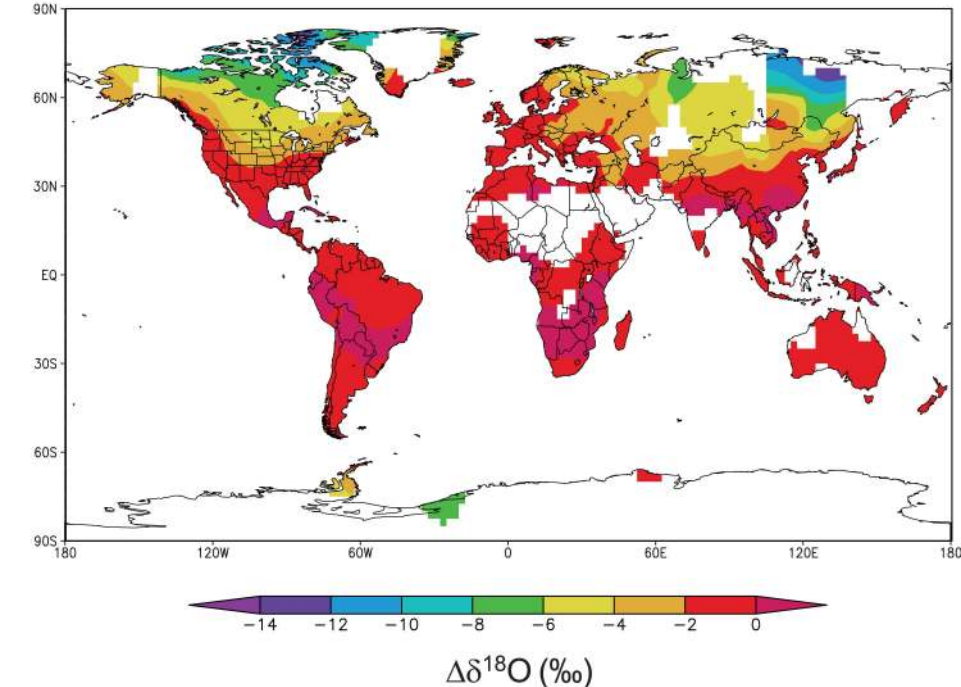
90N
60N
30N
EQ
30S
60S
90S
180
120W
60W
0
60E
120E
180
−14
−12
−10
−8
−6
−4
−2
0
$\Delta\delta^{18}O$ (‰)

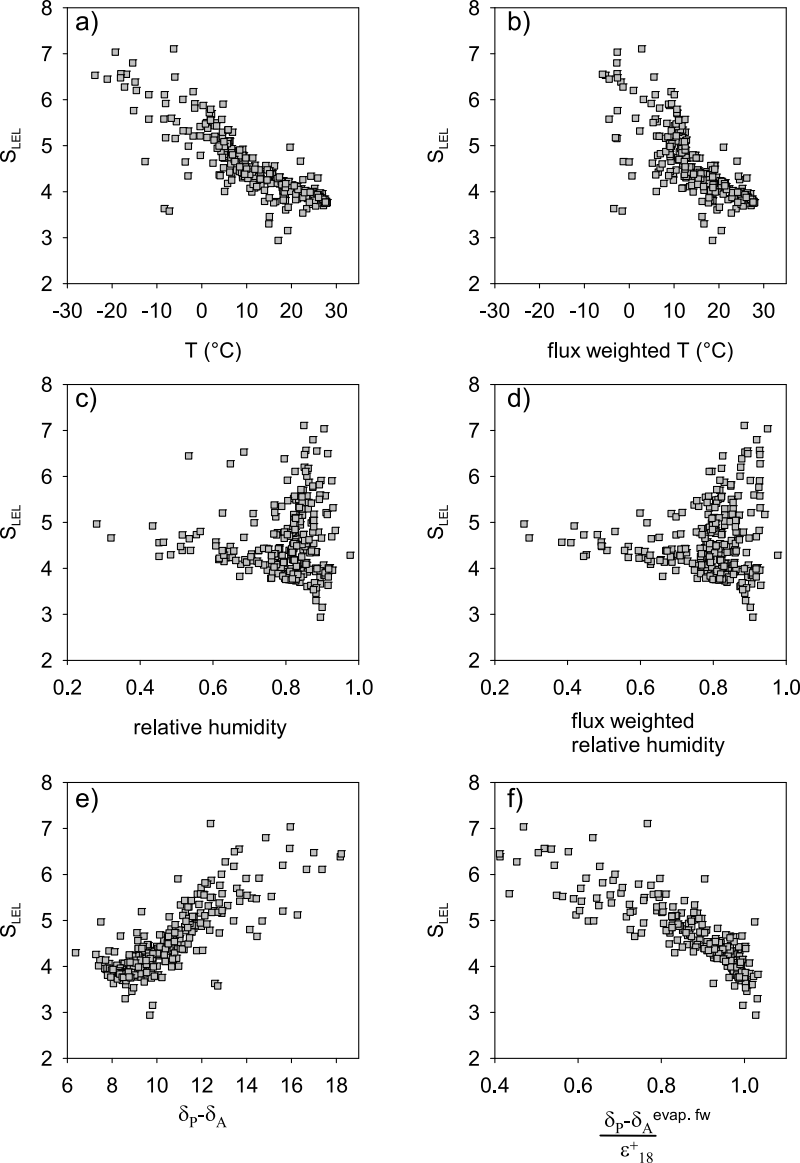
a)
b)
c)
d)
e)
f)
S_{LEL}
T (°C)
flux weighted T (°C)
relative humidity
flux weighted
relative humidity
δ_P-δ_A
$\frac{\delta_P-\delta_A^{evap.\ fw}}{\varepsilon^+_{18}}$

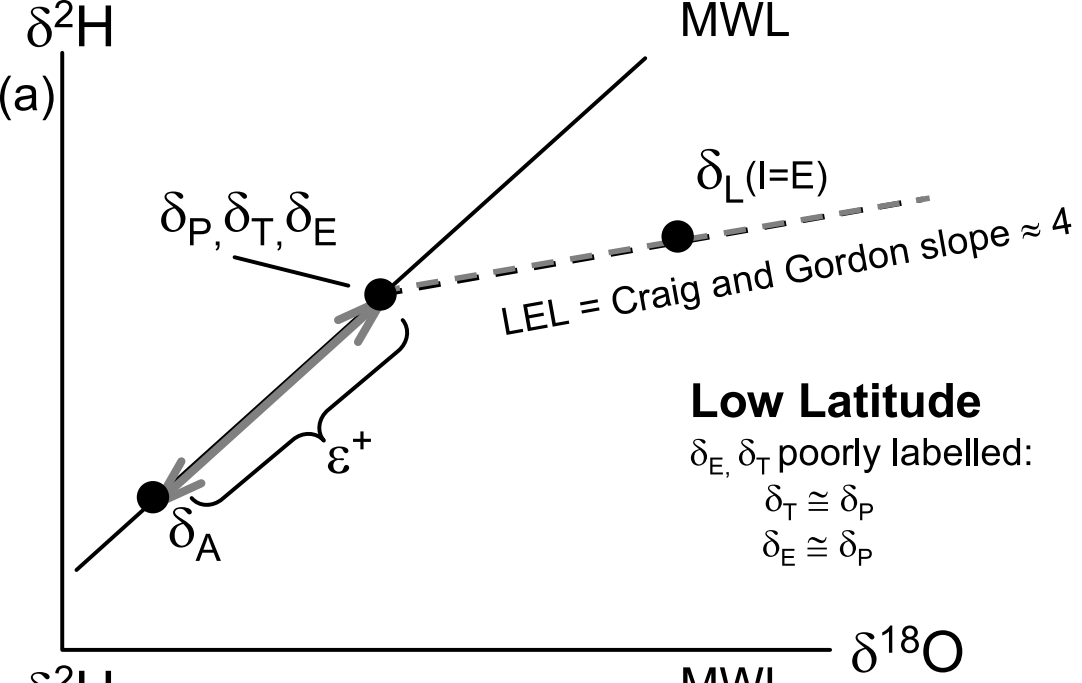
δ2H
MWL
(a)
δL(I=E)
δP,δT,δE
LEL = Craig and Gordon slope ≈ 4
ε+
δA
Low Latitude
δE, δT poorly labelled:
δT ≅ δP
δE ≅ δP
δ18O

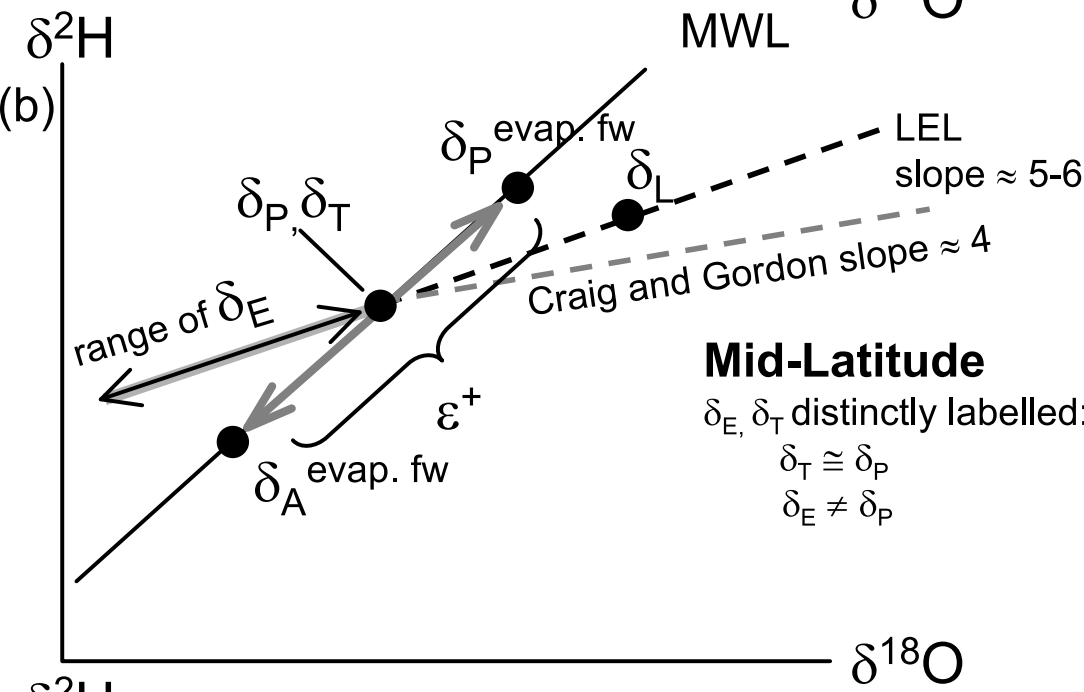
δ2H
MWL
(b)
δP evap. fw
δL
LEL
slope ≈ 5-6
δP,δT
Craig and Gordon slope ≈ 4
range of δE
ε+
δA evap. fw
Mid-Latitude
δE, δT distinctly labelled:
δT ≅ δP
δE ≠ δP
δ18O

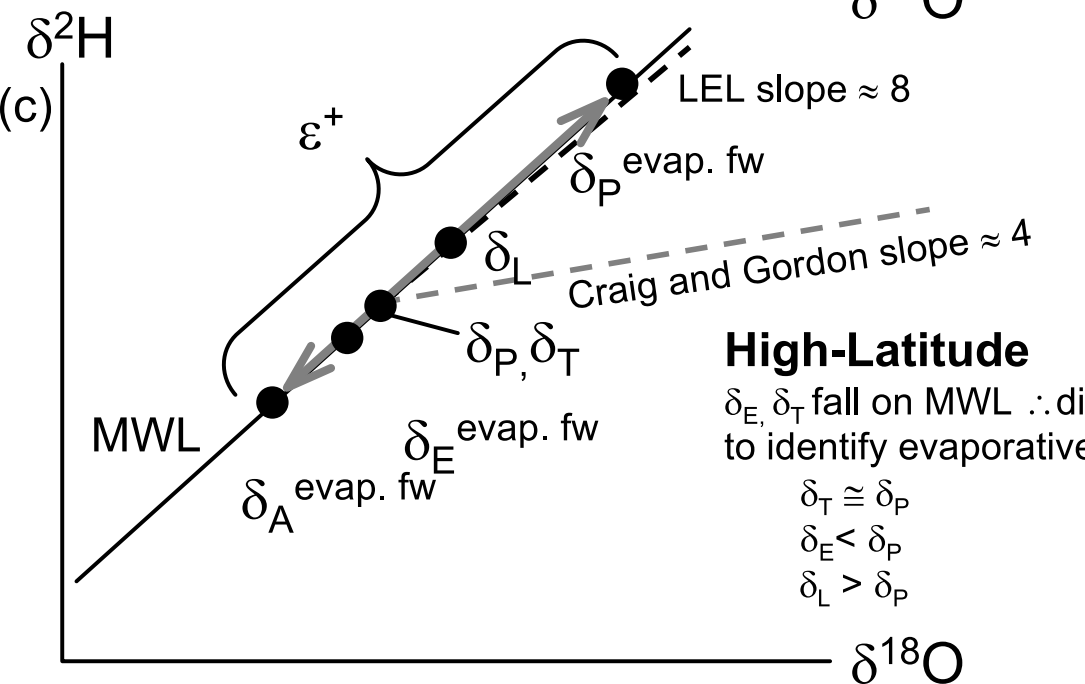
δ2H
(c)
LEL slope ≈ 8
ε+
δP evap. fw
δL
Craig and Gordon slope ≈ 4
δP,δT
MWL
δE evap. fw
δA evap. fw
High-Latitude
δE, δT fall on MWL ∴difficult
to identify evaporative enrichment
δT ≅ δP
δE< δP
δL > δP
δ18O